Low Temperature Physics/Fizika Nizkikh Temperatur, 2020, v. 46, No. 8, pp. 984–990

Wannier–Stark ladder spectrum of Bloch oscillations of magneto-dipole spin waves in graded 1D magnonic crystals

E.V. Tartakovskaya

Institute of Magnetism NAS of Ukraine and MES of Ukraine, Kyiv 03142, Ukraine
E-mail: olena.tartakivska@gmail.com

A.S. Laurenson and V.V. Kruglyak

University of Exeter, Stocker Road, Exeter, EX4 4QL, United Kingdom

Received February 27, 2020, published online June 22, 2020

We have used the method of Wannier functions to calculate the frequencies and profiles of spin waves localized in one-dimensional magnonic crystals due to a gradient in the bias magnetic field. This localization of spin waves is analogous to the phenomenon of Bloch oscillations of quantum-mechanical electrons in crystals in a uniform electric field. As a convenient yet realistic model, we consider backward volume magnetostatic spin waves in a film of yttrium-iron garnet in a bias magnetic field comprising spatially uniform, cosine and gradient contributions. The spin-wave spectrum is shown to have the characteristic form of a Wannier–Stark ladder. The analytical results are verified using those obtained using numerical micromagnetic simulations. The physics of spin-wave Bloch oscillations combines the topics of magnonic crystals and graded magnonic index — the two cornerstones of modern magnonics.

Keywords: spin waves, Bloch oscillations, one-dimensional magnonic crystals.

The concept of elementary excitations is one of the cornerstones of modern physics, including such an important and quickly developing part of it as physics of superlattices and nanostructures. Just as the dynamics of crystal structures is determined by the spectrum of phonons (quanta of normal modes of collective elastic vibrations of atoms), the dynamics of magnetically ordered systems is described using the concept of elementary magnetization excitations — spin waves (SWs) — and their quanta — magnons. SWs determine the high-frequency dynamics and relaxation of the magnetization in magnetic materials, as well as their thermal and kinetic properties [1–5].

The behavior of plane waves in artificial periodic media, e.g., superlattices, is analogous to well-investigated case of electron waves in crystals. For instance, the waves' band structures are similar to the valence and the conduction bands in semiconductors. Hence, after application of the well-developed methods of quantum mechanics and solid-state physics to such new artificially nanostructured materials, properties of elementary excitations in photonic [6,7], acoustic [8,9], and magnonic [10–13] crystals were successfully investigated.

Among other interesting effects, such a well-known phenomenon as Bloch oscillations (localization) [14] is also not unique to electrons in crystals but can occur for any waves in periodic media with graded properties. Bloch oscillations were observed, for instance, in optical (photonic) [15,16] and acoustic (phononic) [17,18] structures. A similar phenomenon was investigated in arrays of cold atoms [19–21] and in the systems with a strong spin-orbit coupling in gradient magnetic field [22,23]. However, neither experimental [24–28] nor theoretical [29–31] investigations did give the evidence of SW localization in realistic magnetic nanostructures with graded properties. Actually, the task of studying Bloch oscillations was not posed in these experimental works, so the temperature [28] and bias magnetic field [24–27] gradients were chosen too small for these oscillations to be detected. As to the theoretical studies, the possibility of existence of Bloch localization in magnetic systems was confirmed in principle, but only for models far from realistic, experimentally realisable magnonic crystals. In Refs. 29 and 32, only nonlinear excitations were considered, whose behavior obeys laws different to those for linear elementary excitations of the SW type. In Refs. 30 and 31,

concrete calculations of the excitations spectra in the form of a Wannier–Stark ladder were performed. However, only discrete models with exchange interactions between spins were considered. Yet, for the sizes of realistic nanostructures, the most suitable is the phenomenological model of a continuous medium dominated by the magneto-dipolar interaction [1,2,33].

In this article, we present results of analytical and numerical calculations that show Bloch oscillations and their spectra in the form of Wannier–Stark ladder for the backward volume magnetostatic spin waves (BVMSWs) in magnonic crystals with realistic sizes and geometry. We consider a thin film of yttrium-iron garnet (YIG) in a bias magnetic field parallel to the film's surface (along the x axis). This external bias magnetic field is a sum of three terms: (1) a spatially uniform term, (2) cosine term (which forms the analogue of superlattice), and (3) a slowly varying linear term. The geometry of the problem is presented in Fig. 1. We assume that the sample is in the saturated state and that the static average magnetization of the film is co-directional with it. We treat the magnetization of the film as the sum of the saturation magnetization and a weakly excited term (i.e., an SW), which has two spatial components $(\mu_y(x), \mu_z(x))\exp(i\Omega t)$.

To find the frequencies of spin waves Ω, we use the Landau–Lifshitz equation,

$$\begin{cases} i\Omega\mu_y(x) = (\omega_H + \omega_h\cdot\cos(Kx) + \gamma\mu_0 Gx)\mu_z(x), \\ -i\Omega\mu_z(x) = (\omega_H + \omega_h\cdot\cos(Kx) + \gamma\mu_0 Gx)\mu_y(x) - \omega_M\hat{h}(\mu_y(x)), \end{cases} \tag{1}$$

where the term $\gamma\mu_0 Gx$ describes the field gradient, $\omega_H = \gamma\mu_0 H$, where H is the spatially uniform component of the magnetic field, M is the saturation magnetization, $\omega_M = \gamma M$, μ_0 is the permeability, γ is the gyromagnetic ratio, a is the period of the cosine static magnetic field, and values $K = 2\pi/a$, and $\omega_h = \gamma\mu_0 h$ correspond to the scale and the amplitude of the field modulation. The dynamical dipolar field is

$$\hat{\mathbf{h}}(\mu_y) = -\frac{\partial}{\partial y}\int d\mathbf{r}'(\mu_y\cdot\nabla')\frac{1}{|\mathbf{r}-\mathbf{r}'|}. \tag{2}$$

If $G = 0$, the solution of Eq. (1) is a standard linear eigenfrequency and eigenfunction problem. In this case, we denote the SW solutions as $m_y(k,x)$ and $m_z(k,x)$, and corresponding frequencies as $\omega(k)$. In accordance with the Bloch theorem for a periodic potential, we can employ the usual for magnonics, photonics and phononics presentation for elementary excitations, representing the two SW components as

$$\begin{aligned} m_y(k,x) &= e^{-ikx}\sum_n T_n(k)\exp\left(i\frac{2\pi n}{a}x\right), \\ m_z(k,x) &= e^{-ikx}\sum_n D_n(k)\exp\left(i\frac{2\pi n}{a}x\right). \end{aligned} \tag{3}$$

Setting $G = 0$ in Eq. (1), we obtain an infinite system of linear algebraic equations for coefficients $D_n(k)$ and $T_n(k)$

$$\begin{cases} i\omega(k)T_n(k) = \omega_H D_n(k) + \dfrac{\omega_h}{2}(D_{n+1}(k) + D_{n-1}(k)), \\ -i\omega(k)D_n(k) = \Xi_n(k)T_n(k) + \dfrac{\omega_h}{2}(T_{n+1}(k) + T_{n-1}(k)), \end{cases} \tag{4}$$

where

$$\Xi_n(k) = \left(\omega_H + \omega_M\frac{1-\exp\left(-\left|k-\frac{2\pi n}{a}\right|d\right)}{\left|k-\frac{2\pi n}{a}\right|d}\right). \tag{5}$$

We consider the case when $\omega_h/\omega_H << 1$. This allows us to approximate the full solution of the problem Eqs. (4), (5) by a finite-sized subset of the basis states and leads to the standard diagonalization of the characteristic matrix of finite size for Eq. (4). As a result, we obtain the expected picture of the band dispersion $\omega(k)$, which is usual for crystals.

The magnonic bands are ordered in frequency from top to down. As our numerical calculations show (Fig. 2, black dash lines), with parameters chosen here the periodic field modulation induces a large first band gap, while the other (higher order) band gaps are significantly smaller and the

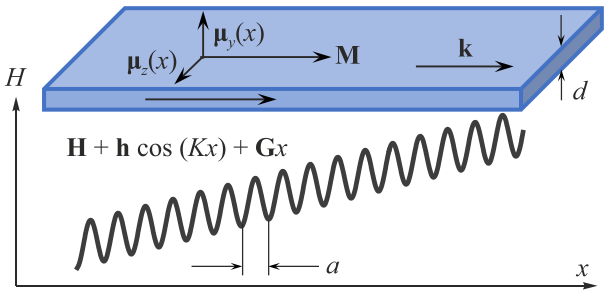

Fig. 1. The geometry of the problem is shown. A thin magnetic film of thickness d is magnetised along the x axis by a bias magnetic field comprising spatially uniform H, cosine $h\cos(Kx)$, and gradient $\mathbf{G}x$ contributions. SWs propagate (with a wave vector $\mathbf{k}$) also along the x axis (BVMSW geometry). The period of the cosine field contribution is a =3 μm, and so, $K = 2\pi/a$.

allowed bands are increasingly flat. So, we can try to limit our model to the first and second bands only. In this approximation, the characteristic equation takes the following simple biquadratic form

$$\left(\omega(k)^2-\left[\omega_H\Xi_0+\frac{\omega_h^{\,2}}{2}\right]\right)\left(\omega(k)^2-\left[\omega_H\Xi_1+\frac{\omega_h^{\,2}}{2}\right]\right)-\left[\Xi_1+\omega_H\right]\left[\Xi_0+\omega_H\right]\frac{\omega_h^{\,2}}{4}=0. \quad (6)$$

The magnonic dispersion relations for the first, $\omega_+(k)$, and second, $\omega_-(k)$, bands can be found analytically as

$$\omega_\pm(k)=\sqrt{\frac{1}{2}\left\{\left[\omega_H\left(\Xi_0+\Xi_1\right)+\omega_h^{\,2}\right]\pm\sqrt{\omega_H^{\,2}\left(\Xi_0-\Xi_1\right)^2+\left(\omega_H\left(\Xi_0+\Xi_1\right)+\Xi_1\Xi_0+\omega_H^{\,2}\right)\omega_h^{\,2}}\right\}}. \quad (7)$$

Using Eq. (7), we can find the analytical expression for the gap Δ_{gap} between the first and the second bands as

$$\Delta_{\text{gap}}=\omega_+\left(\frac{\pi}{a}\right)-\omega_-\left(\frac{\pi}{a}\right)\approx\sqrt{\frac{\omega_H}{\Xi}}\left(\Xi+\omega_H\right)\frac{\omega_h}{2\omega_H}, \quad (8)$$

where $\Xi=\Xi_0(\pi/a)=\Xi_1(\pi/a)$. In the first approximation by the small parameter ω_h/ω_H, the band gap is linear in ω_h/ω_H.

Figure 2 shows the magnonic dispersion relations in the first Brillouin zone, calculated for a uniform bias magnetic field of 185 mT spatially modulated by an additional cosine static magnetic field with a period of 3 μm. The calculations are shown for different amplitudes of the field modulations: panels (a) and (b) correspond to the field amplitudes of $\mu_0 h$ = = 5 mT and $\mu_0 h$ = 10 mT, respectively. The SW branches are calculated for two different finite-sized subsets of the basic states: numerically with the extended scheme by Eqs. (4), (5), shown by black dashed lines, and analytically for the first two bands by Eq. (7), shown by red solid lines. As expected, the analytical result gives a good approximation in the case of $\mu_0 h$ = 5 mT, while the discrepancy between analytical and numerical calculations increases for $\mu_0 h$ = 10 mT.

At the next step, we use the eigenvalues $\omega(k)$ given by Eq. (7) and the corresponding eigenfunctions $m_y(k,x)$, $m_z(k,x)$ given by Eq. (3) calculated for $G=0$ to construct solutions of the problem with a nonzero field gradient. So, we return to Eq. (1) with $G\neq 0$. Our task is to find new eigenvalues Ω and new eigenfunctions, $\mu_y(x)$ and $\mu_z(x)$. Now the magnetic excitations in the sample cannot be presented in the form of the expansion (3). Indeed, firstly, such a representation is a consequence of the Bloch theorem, i.e., of the periodicity of the potential, while this periodicity is broken when the gradient is nonzero. Secondly, the matrix elements of the new graded potential proportional to Gx diverge if the eigenfunctions are not localized. So, we must use basis functions that are localized in the real space. In this case, Wannier functions [34,35] are a good choice.

The scheme common in the problem of electron localization in crystals in a uniform electric field is applied to one band with an assumption of non-interacting bands. Due to the large first band gap in our magnonic crystal, an

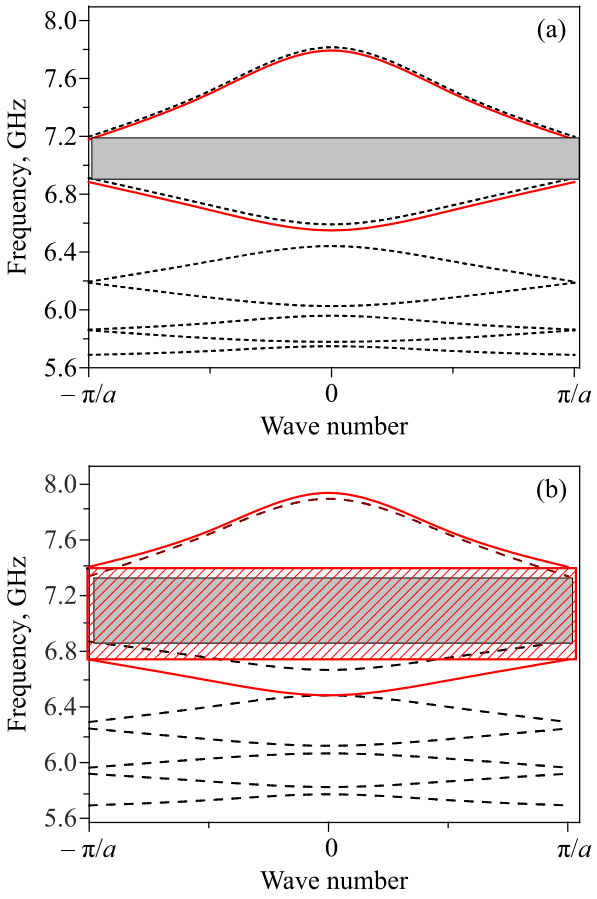

Fig. 2. (Color online) The SW frequency is shown as a function of the wave number in the first Brillouin zone. The cosine static magnetic field with a period of 3 μm has the modulation amplitude of $\mu_0 h$ = 5 mT (a) and $\mu_0 h$ = 10 mT (b). The black dash lines show the calculations by Eqs. (4), (5) with the indices n varying from 0–10 (only the first 7 bands are shown). The red solid lines show the analytical calculations by Eq. (7), i.e., n = 0,1. The grey stripe in panel (a) shows the first band gap, which is almost the same in the two approximations. The grey stripe and the red hatched stripe in (b) show the first band gap for numerical and analytical calculations, respectively. Both in panels (a) and (b), the uniform bias magnetic field is $\mu_0 H$ = 185 mT, the saturation magnetization is M = 200 kA / m, $\gamma/2\pi$ = 28 GHz/T, and the film thickness is d =1 μm.

interband tunnelling between the first and second band is negligible, which allows us to find the Wannier–Stark ladder spectrum in the isolated first band.

We determine two sets of Wannier functions for both components of the SW in the usual way

$$a(x-R)=\frac{a}{2\pi}\int\limits_{-\pi/a}^{\pi/a} dk\, e^{ikR} m_y(k,x),$$

$$b(x-R)=\frac{a}{2\pi}\int\limits_{-\pi/a}^{\pi/a} dk\, e^{ikR} m_z(k,x), \qquad (9)$$

where $m_y(k,x)$ and $m_z(k,z)$ are the solutions (3) of the eigenproblem with $G=0$, described above. $R_n = n\cdot a$, where n are integers, are coordinates of the external field maxima, which are analogues of the atomic positions in a crystal. The Wannier functions have sharp extrema near the corresponding R (Fig. 3a). This is the source of orthogonality of Wannier functions

$$\int dx a(x-R')a^*(x-R) = f\Delta(R-R'),$$

$$\int dx b(x-R')b^*(x-R) = g\Delta(R-R'),$$

$$\int dx a(x-R')b^*(x-R) = s\Delta(R-R'), \qquad (10)$$

which we employ below. It follows from Eqs. (1), (4) and (9) that constants f and g are real, while constant s is imaginary.

Further, we represent unknown profiles $\mu_x(z)$ and $\mu_y(z)$ as superpositions of Wannier functions (9):

$$\mu_y(x)=\sum_R A(R)a(x-R),$$

$$\mu_z(x)=\sum_R B(R)b(x-R). \qquad (11)$$

To obtain the coefficients $A(R)$ and $B(R)$, we substitute Eq. (11) into Eq. (1). At the length scale of variation of Wannier functions, $Gx \approx GR$, and so, integrating both parts of the equations by x and using Eq. (10), we rewrite Eq. (1) as

$$\begin{cases} i\Omega f A(R) = i\dfrac{a}{2\pi}\displaystyle\int\limits_{-\pi/a}^{\pi/a} dk\, e^{-ikR} B(k)\omega_+(k) + \gamma\mu_0 GRB(R)\cdot s^*, \\ -i\Omega g B(R) = -i\dfrac{a}{2\pi}\displaystyle\int\limits_{-\pi/a}^{\pi/a} dk\, e^{-ikR} A(k)\omega_+(k) + \gamma\mu_0 GRA(R)\cdot s, \end{cases} \qquad (12)$$

where $\omega_+(k)$ is determined by Eq. (7).

In k-representation, Eq. (12) takes the following form

$$\begin{cases} \Omega A(k) = B(k)\omega_+(k) - \gamma\mu_0 G\dfrac{s^*}{f}\dfrac{\partial}{\partial k}B(k), \\ \Omega B(k) = A(k)\omega_+(k) + \gamma\mu_0 G\dfrac{s}{g}\dfrac{\partial}{\partial k}A(k). \end{cases} \qquad (13)$$

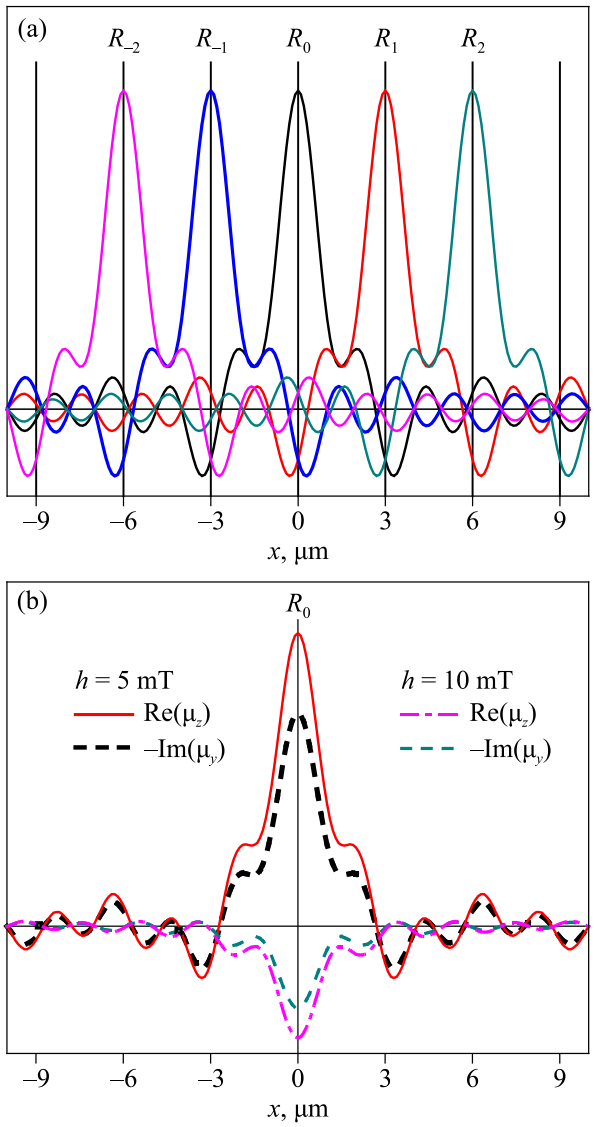

Fig. 3. (Color online) (a) Examples of Wannier functions $b(x-R_i)$ centred around the R_i ($i=0,\pm1,\pm2$) points, calculated using Eq. (9), are shown for $\mu_0 h$ = 10 mT, $\mu_0 H$ = 185 mT, a = 3 μm, d = 1 μm, M = 200 kA/m. (b) The profiles of localized SWs, calculated using Eqs. (11), (14) for the central level $\Omega_0 \approx \sqrt{\langle \omega_+^2 \rangle}$ of the corresponding Wannier–Stark ladder $\mu_0 h$ = = 5 mT – red (Re(μ_z)) and dash black (–Im(μ_y)) lines, $\mu_0 h$ = = 10 mT – dash-dot magenta (Re(μ_z)) and dash green (–Im(μ_y)) lines), are shown for a field gradient of $\mu_0 G$ = 40 mT/mm.

From Eq. (13), we obtain an equation for one of the unknown functions, for instance, for $A(k)$

$$\Omega^2 A(k) = A(k)\big(\omega(k)\big)^2 + \left\{\frac{s}{g}-\frac{s^*}{f}\right\}\gamma\mu_0 G\Omega\frac{\partial}{\partial k}A(k). \qquad (14)$$

This is a differential equation of the first order with constant coefficients, and so, it has a standard solution:

$$A(k) = \tilde{A}\exp\left(\frac{i}{\gamma\mu_0 G\alpha}\int_0^k \frac{\Omega^2 - \left(\omega_+(k')\right)^2}{\Omega}dk'\right), \quad (15)$$

where $\alpha = -Im\left\{\frac{s}{g} - \frac{s^*}{f}\right\}$.

The dispersion relation can be found from the periodic boundary condition

$$A(k) = A\left(k + \frac{2\pi}{a}n\right), \quad (16)$$

where n are integer. From Eqs. (15) and (16), we obtain a quadratic equation

$$\Omega^2 - \Omega \cdot n \cdot Ga\gamma\alpha - \left\langle \omega_+^2 \right\rangle = 0, \quad (17)$$

where $\left\langle \omega_+^2 \right\rangle = \frac{a}{\pi}\int_0^{\pi/a} \left(\omega_+(k')\right)^2 dk'$.

The solution of Eq. (17) is

$$\Omega_n = \frac{1}{2}\left[n \cdot \gamma\mu_0 Ga\alpha + \sqrt{(n \cdot \gamma\mu_0 Ga\alpha)^2 + 4\left\langle \omega_+^2 \right\rangle}\right],$$

which can be written in the form of the Wannier–Stark ladder,

$$\Omega_n \approx \sqrt{\left\langle \omega_+^2 \right\rangle} + \frac{1}{2}n \cdot \gamma\mu_0 Ga\alpha, \quad (18)$$

if the gradient of external magnetic field is small enough, i.e., $(\gamma\mu_0 Ga\alpha)^2 \ll 4\left\langle \omega_+^2 \right\rangle$.

Equation (18) shows that an energy band of a magnonic crystal, with initial dispersion relation $\omega_+(k)$, in a weakly graded field gives rise to the Wannier–Stark ladder with central level $\Omega_0 \approx \sqrt{\left\langle \omega_+^2 \right\rangle}$ and the distance between levels $\frac{1}{2}\gamma\mu_0 Ga\alpha$. For instance, the Wannier–Stark ladder in the first band, as calculated using Eq. (18) for $\mu_0 G$ = 40 mT/mm and $\mu_0 h$ = 5mT, consists of a set of levels with the central level at $\Omega_0 \approx 7.498$ GHz and with the distance between

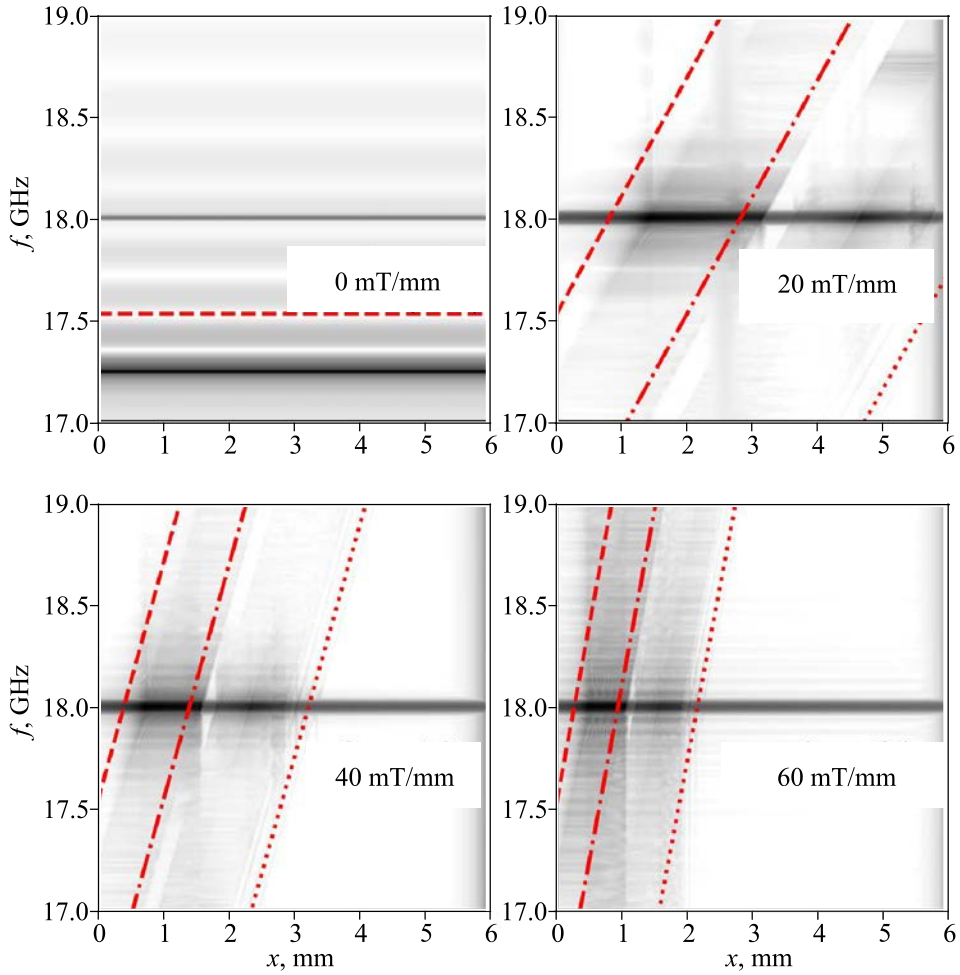

Fig. 4. Spatial maps of the SW amplitude distribution are shown for $\mu_0 h$ = 10 mT, $\mu_0 H$ = 0.5 T, a = 3 μm, d = 1 μm, and M = 200 kA/m and the indicated values of the magnetic field gradient. The greyscale shows the results of the numerical simulations (darker color corresponds to greater Fourier amplitude of spin waves). The dashed and dotted lines show the top and bottom boundaries of the whole BVMSW band in a uniform film, while the dash-dotted line corresponds to the bottom edge of the first magnonic band estimated from the empty-lattice approximation.

neighbouring levels δ of about 3.6 MHz. For the amplitude of the field modulation of $\mu_0 h$ = 10mT and the same field gradient, these values become $\Omega_0 \approx 7.586$ GHz and $\delta \approx$ ≈ 3.45 MHz. Figure 3b shows profiles of localized SWs that corresponding to the central level of the Wannier–Stark ladder and the two values of the amplitude of the field modulation.

The results of the analytical theory presented above are in agreement with those obtained from micromagnetic simulations performed using MuMax software [36]. The simulations are run in the time domain and their results are converted into the frequency domain using standard Fourier techniques [37]. Figure 4 shows the spatial maps of the SW amplitude distributions for different value so the magnetic field gradient and excitation by a uniform microwave magnetic field with a spectrum centred at 18 GHz and spectral bandwidth of 10 MHz. This microwave field couples to the magnetization precession where the frequency matches either uniform ferromagnetic resonance (FMR) frequency (at about 17.2 GHz) or that corresponding to the band edges in the Brillouin zone centre, i.e. $k = 2\pi n / a$, where n is an integer number. At zero gradient, only the FMR mode is excited and then very weakly. At finite values of the field gradient, the Wannier–Stark ladder spectrum is formed. However, the individual levels are not very well resolved, owing to the very small frequency splitting between the neighbouring levels.

In summary, we have used analytical theory based on the method of Wannier functions and numerical simulations to study the spectrum of BVMSW in magnonic crystals subjected to a graded magnetic field. Our results demonstrate that this field gradient can lead to Bloch oscillations of localized SWs, with their spectrum having the characteristic form of the Wannier–Stark ladder. Here, we have presented results for magnonic crystals formed by applying using a cosine-modulated bias magnetic field to a thin film of YIG. Strictly speaking, such a bias magnetic field does not satisfy one of the Maxwell equations, $\mathrm{div}\,\mathbf{B} = 0$. The account of a corresponding out-of-plane non-uniform bias magnetic field, which would ensure that the equation is satisfied, does not change substantially our theory. Moreover, the field should be treated as a general effective magnetic field, representing, e.g., modulated anisotropy or exchange bias [38]. We have also performed similar calculations and obtained similar results for other 1D magnonic crystals, e.g., those formed by arrays of long rectangular strips. The calculations can be generalised to other SW geometries, to the case of dipole-exchange SWs, to graded magnonic crystals formed via spatial modulation (periodic and linear) of the magnonic index through other mechanisms [39], and to the case of a spatial variation of the lattice constant a.

The research leading to these results has received funding from the Engineering and Physical Sciences Research Council of the United Kingdom, via the EPSRC Centre for Doctoral Training in Metamaterials (Grant No. EP/L015331/1), and from the European Union's Horizon 2020 research and innovation program under Marie Skłodowska-Curie Grant Agreement No. 644348 (MagIC). The authors also gratefully acknowledge valuable discussions with J. Bertolotti, Y.I. Gorobets, and B.A. Ivanov.

1. A.I. Akhiezer, V.G. Bar'yakhtar, and M.I. Kaganov, *Usp. Fiz. Nauk* **71**, 533 (1960) [A.I. Akhiezer, V.G. Bar'yakhtar, and M.I. Kaganov, *Sov. Phys. Usp.* **3**, 567 (1960)].
2. A.I. Akhiezer, V.G. Bar'yakhtar, and S.V. Peletminskii, *Spin Waves*, John Wiley & Sons, North-Holland, Amsterdam (1968).
3. V.G. Bar'yakhtar and S.V. Maleev, *J. Exper. Theor. Phys.* **39**, 1430 (1960) [*Sov. Phys. JETP* **12**, 995 (1961)].
4. V.G. Bar'yakhtar, B.A. Ivanov, and M.V. Chetkin, *Usp. Fiz. Nauk* 146, 417 (1985).
5. V.G. Bar'yakhtar, *The Phenomenological Theory of Relaxation Processes in Magnets*, in: *Frontiers in Magnetism of Reduced Dimension Systems*, V.G. Bar'yakthar, P.E. Wigen, and N.A. Lesnik (eds.), *NATO ASI Series*, Springer, Dordrecht (1998), Vol. 49.
6. E. Yablonovitch, *J. Phys. Condens. Matter* **5**, 2443 (1993).
7. N. Kumar and B. Suthar, *Advances in Photonic Crystals and Devices*, CRC Press, Boca Raton (2019).
8. M.S. Kushwaha, P. Halevi, G. Martínez, L. Dobrzynski, and B. Djafari-Rouhani, *Phys. Rev. B* **49**, 2313 (1994).
9. E.V. Tartakovskaya, *Phys. Rev. B* **62**, 11225 (2000).
10. M. Krawczyk, J.-C. Lévy, D. Mercier, and H. Puszkarski, *Phys. Lett. A* **282**, 186 (2001).
11. V.V. Kruglyak, S.O. Demokritov, and D. Grundler, *J. Phys. D* **43**, 264001 (2010).
12. M. Krawczyk and D. Grundler, *J. Phys. Condens. Matter* **26**, 123202 (2014).
13. V.V. Kruglyak, C.S. Davies, V.S. Tkachenko, O.Y. Gorobets, Y.I. Gorobets, and A.N. Kuchko, *J. Phys. D* **50**, 094003 (2017).
14. F. Bloch, *Zeitschrift für Physik* **52**, 555 (1929).
15. R. Sapienza, P. Costantino, D. Wiersma, M. Ghulinyan, C.J. Oton, and L. Pavesi, *Phys. Rev. Lett.* **91**, 263902 (2003).
16. V. Agarwal, J.A. del Río, G. Malpuech, M. Zamfirescu, A. Kavokin, D. Coquillat, D. Scalbert, M. Vladimirova, and B. Gil, *Phys. Rev. Lett.* **92**, 097401 (2004).
17. N. Lanzillotti-Kimura, A. Fainstein, B. Perrin, B. Jusserand, O. Mauguin, L. Largeau, and A. Lemaître, *Phys. Rev. Lett.* **104**, 197402 (2010).
18. M.M. de Lima, Jr., Y.A. Kosevich, P.V. Santos, and A. Cantarero, *Phys. Rev. Lett.* **104**, 165502 (2010).
19. M. Ben Dahan, E. Peik, J. Reichel, Y. Castin, and C. Salomon, *Phys. Rev. Lett.* **76**, 4508 (1996).
20. S.R. Wilkinson, C.F. Bharucha, K.W. Madison, Q. Niu, and M.G. Raizen, *Phys. Rev. Lett.* **76**, 4512 (1996).
21. Q. Niu, X.-G. Zhao, G.A. Georgakis, and M.G. Raizen, *Phys. Rev. Lett.* **76**, 4504 (1996).
22. Y. Ke, X. Qin, H. Zhong, J. Huang, C. He, and C. Lee, *Phys. Rev. A* **91**, 053409 (2015).
23. Y.V. Kartashov, V.V. Konotop, D.A. Zezyulin, and L. Torner, *Phys. Rev. Lett.* **117**, 215301 (2016).

24. A.V. Vashkovskii and E.G. Lokk, *J. Commun. Technol. Electron.* **46**, 1163 (2001).
25. K.R. Smith, M.J. Kabatek, P. Krivosik, and M. Wu, *J. Appl. Phys.* **104**, 344002 (2008).
26. V.E. Demidov, M.P. Kostylev, K. Rott, J. Munchenberger, G. Reiss, and S.O. Demokritov, *Appl. Phys. Lett.* **99**, 082507 (2011).
27. N. Perez and L. Lopez-Diaz, *Phys. Rev. B* **92**, 014408 (2015).
28. T. Langner, D.A. Bozhko, S.A. Bunyaev, G.N. Kakazei, A.V. Chumak, A.A. Serga, B. Hillebrands, and V.I. Vasyuchka, *J. Phys. D* **51**, 344002 (2018).
29. A.M. Kosevich, *Fiz. Nizk. Temp.* **27**, 699 (2001) [*Low Temp. Phys.* **27**, 513 (2001)].
30. V.V. Gann and Y.A. Kosevich, *Fiz. Nizk. Temp.* **36**, 909 (2010) [*Low Temp. Phys.* **36**, 722 (2010)].
31. G. Monsivais and C.L. Ordóñez-Romero, *J. Magn. Magn. Mater.* **466**, 150 (2018).
32. E.G. Galkina, B.A. Ivanov, S. Savel'ev, and F. Nori, *Phys. Rev. B* **77**, 134425 (2008).
33. M. Pardavi-Horvath, *Phys. Status Solidi A* **211**, 1030 (2014).
34. G.H. Wannier, *Rev. Mod. Phys.* **34**, 645 (1962).
35. J.M. Ziman, *Principles of the Theory of Solids*, Cambridge University Press (1972).
36. A. Vansteenkiste, J. Leliaert, M. Dvornik, M. Helsen, F. Garcia-Sanchez, and B. Van Waeyenberge, *AIP Adv.* **4**, 107133 (2014).
37. M. Dvornik, Y. Au, and V.V. Kruglyak, *Top. Appl. Phys.* **125**, 101 (2013).
38. Y.I. Gorobets, A.E. Zyubanov, A.N. Kuchko, and K.D. Shedzhuri, *Fiz. Tverd. Tela* **34**, 1486 (1992).
39. C.S. Davies and V.V. Kruglyak, *Fiz. Nizk. Temp.* **41**, 976 (2015) [*Low Temp. Phys.* **41**, 760 (2015)].

Спектр Ваньє-Старка блохівських коливань магнітодіпольних спінових хвиль у градієнтних одновимірних магнонних кристалах

О.В. Тартаковська, A.S. Laurenson, V.V. Kruglyak

Використано метод функцій Ваньє для розрахунку частот та профілів спінових хвиль, які локалізовані в одновимірних магнонних кристалах завдяки градієнту поля, яке підмагнічує. Така локалізація спінових хвиль аналогічна появі блохівських коливань квантово-механічних електронів у кристалах в однорідному електричному полі. Розглянуто модель магнітостатичних зворотних об'ємних спінових хвиль у плівці залізо-ітрієвого гранату у полі підмагнічення, що включає просторово однорідний, косинусний та градієнтний внески. Показано, що спектр спінових хвиль має характерну форму сходів Ваньє–Старка. Результати аналізів перевірено з використанням результатів, які отримано за допомогою чисельного мікромагнітного моделювання. Фізика блохівських коливань спінових хвиль об'єднує дослідження магнонних кристалів та градієнтного магнонного індексу — двох фундаментальних основ сучасної магноніки.

Ключові слова: спінові хвилі, блохівські коливання, одновимірні магнонні кристали.